

การยับยั้งฟอสฟอริเลชันของสารประกอบเชิงซ้อนไซคลินดีเพนเดนตีโคเนส 6/ไซคลินดี
ด้วยฟลาโวนอยด์โดยการจำลองพลวัตเชิงโมเลกุล

นางสาววาสนี ขุนทวี

วิทยานิพนธ์นี้เป็นส่วนหนึ่งของการศึกษาตามหลักสูตรปริญญาวิทยาศาสตรมหาบัณฑิต

สาขาวิชาเคมี ภาควิชาเคมี

คณะวิทยาศาสตร์ จุฬาลงกรณ์มหาวิทยาลัย

ปีการศึกษา 2553

ลิขสิทธิ์ของจุฬาลงกรณ์มหาวิทยาลัย

PHOSPHORYLATION INHIBITION OF CYCLIN DEPENDENT KINASE 6/CYCLIN D
COMPLEX WITH FLAVONOIDS USING MOLECULAR DYNAMICS SIMULATIONS

Miss Wasinee Khuntawee

A Thesis Submitted in Partial Fulfillment of the Requirements
for the Degree of Master of Science Program in Chemistry

Department of Chemistry

Faculty of Science

Chulalongkorn University

Academic Year 2010

Copyright of Chulalongkorn University

วาสิณี ขุนทวี: การยับยั้งฟอสฟอริเลชันของสารประกอบเชิงซ้อนไซคลินดีเพนเดนต์ไคเนส6/ไซคลินดีด้วยฟลาโวนอยด์โดยการจำลองพลวัตเชิงโมเลกุล (PHOSPHORYLATION INHIBITION OF CYCLIN DEPENDENT KINASE 6/CYCLIN D COMPLEX WITH FLAVONOIDS USING MOLECULAR DYNAMICS SIMULATIONS) อ.ที่ปรึกษาวิทยานิพนธ์หลัก: ศ.ดร. สุพจน์ หารหนองบัว, อ.ที่ปรึกษาวิทยานิพนธ์ร่วม: ดร. ธัญญา รุ่งโรจน์มงคล, 32 หน้า.

เป็นที่ยอมรับกันว่าไซคลินดีเพนเดนต์ไคเนส (CDK) ซึ่งทำงานร่วมกับไซคลิน มีบทบาทสำคัญต่อการควบคุมวัฏจักรเซลล์ ในขั้นตอนการอะพอโทซิส และการถ่ายทอดสารพันธุกรรม สารประกอบเชิงซ้อนไซคลินดีเพนเดนต์ไคเนส 6 กับไซคลินดี (CDK6/v) ทำหน้าที่ผลักดันให้เกิดการแบ่งเซลล์ โดยผ่านปฏิกิริยาฟอสฟอริเลชัน เพื่อทำความเข้าใจการยับยั้งของฟลาโวนอยด์ซึ่งเป็นสารยับยั้งของไซคลินดีเพนเดนต์ไคเนส 6 (CDK6) ในตำแหน่งออกฤทธิ์ ดังนั้นในงานวิจัยนี้จึงได้ศึกษาการจำลองพลวัตเชิงโมเลกุลของสารประกอบฟลาโวนอยด์ 3 ชนิด ซึ่งเกิดสารประกอบเชิงซ้อนกับ CDK6/v ใน 4 รูปแบบ คือ ฟิเซอติน (FST-CDK6/v) อะพิจินีน (AGN-CDK6/v) ไครซิน (CHS_A-CDK6/v) และไครซิน (CHS_B-CDK6/v) ผลการศึกษาพบว่าในทุกระบบเกิดพันธะไฮโดรเจนระหว่างหมู่ลิโอดินตำแหน่งที่ 4 ของสารยับยั้งกับไนโตรเจนในโครงสร้างหลักของ V101 และพบว่าไฮดรอกซิลที่ตำแหน่ง 3' และ 4' ของสารยับยั้งมีความสำคัญซึ่งส่งผลให้ประสิทธิภาพของสารยับยั้งเพิ่มขึ้น ความแข็งแรงของพันธะไฮโดรเจนจะแสดงด้วยค่าพลังงานไฟฟ้าสถิต และ ค่าพลังงานเวน เดอร์วาล์ว นอกจากนี้ยังพบว่าอันตรกิริยาที่เกิดกับ I19 V27 F98 H100 และ L152 เป็นปัจจัยที่มีผลต่อประสิทธิภาพการยับยั้งของสารยับยั้ง ทั้งนี้ลำดับของการยับยั้งของสารประกอบฟลาโวนอยด์ทั้ง 3 ชนิดใน 4 รูปแบบที่แสดงด้วยค่าประสิทธิภาพการยึดจับ MM-PBSA เป็นดังนี้ FST-CDK6/v > AGN-CDK6/v > CHS_A-CDK6/v ~ CHS_B-CDK6/v ซึ่งสอดคล้องเป็นอย่างดีกับค่า IC_{50} จากการทดลอง นอกจากนี้ยังพบว่า CHS_B-CDK6/v เป็นโครงสร้างที่มีการยึดจับได้ดีกว่าโครงสร้าง CHS_A-CDK6/v

ภาควิชาเคมี.....ลายมือชื่อนิสิต.....
 สาขาวิชา.....เคมี.....ลายมือชื่อ อ.ที่ปรึกษาวิทยานิพนธ์หลัก.....
 ปีการศึกษา2553.....ลายมือชื่อ อ.ที่ปรึกษาวิทยานิพนธ์ร่วม.....

5272534223 : MAJOR CHEMISTRY

KEYWORDS : CDK6/ FLAVONOID / MOLECULAR DYNAMICS SIMULATION

WASINEE KHUNTAWE: PHOSPHORYLATION INHIBITION OF CYCLIN DEPENDENT KINASE 6/CYCLIN D COMPLEX WITH FLAVONOIDS USING MOLECULAR DYNAMICS SIMULATIONS. ADVISOR: PROFESSOR SUPOT HANNONGBUA, DR. RER. NAT., CO-ADVISOR: THANYADA RUNGROTMONGKOL, Ph.D., 32 pp.

The cyclin dependent kinase (CDK) with an association partner cyclin are known to play an important role on the regulation of the cell cycle, apoptosis and transcription. The cyclin dependent kinase 6 (CDK6) with regulatory cyclin D (CDK6/v) drives cellular proliferation by phosphorylation reaction. To understand the CDK6 inhibitors *i.e.*, flavonoids blocking the CDK6/Cyclin D at ATP binding pocket, MD simulations were performed on three flavonoid inhibitors complexed with CDK6/cyclin D in the four orientations, fisetin (FST-CDK6/v), apigenin (AGN-CDK6/v), chrysin (CHS_A-CDK6/v) and chrysin (CHS_B-CDK6/v). In all systems, the conserved strong H-bond at the 4-keto group of inhibitors via the backbone nitrogen of V101 was found. The 3'- and 4'-OH groups on the B ring were found to significantly increase in binding and inhibitory efficiency. The electrostatics interaction particularly the hydrogen bond formation, the vdW interactions with the I19, V27, F98, H100 and L152 were also found to increase in binding efficiency. The order of the predicted inhibitory affinities base on MM/PBSA approach of these four complexes are FST-CDK6/v > AGN-CDK6/v > CHS_A-CDK6/v ~ CHS_B-CDK6/v which is in good agreement with the experimental data (IC_{50}). Moreover, the CHS_B-CDK6/v is the preferentially bind in the binding site.

Department :Chemistry..... Student's Signature

Field of Study :Chemistry..... Advisor's Signature

Academic Year :2010..... Co-advisor's Signature

ACKNOWLEDGEMENTS

Firstly, I would also like to thank my parent and my family, whose encouraging and understanding and provided me through my entire life and in particular. I would like to express my sincere thanks to my supervisor, Professor Supot Hannongbua, Dr. rer. Nat. for give me an opportunity, excellent suggestions and for his invaluable help throughout the course of this research. I am most grateful for his teaching and advice, not only the research idea but also many other idea in life.

In addition, I am grateful for lovely help and well suggestions from Dr. Thanyada Rungrotmongkol, my co-advisor who helps me from the beginning until this thesis be completed. I would like to give special thanks to all members of Computational Chemistry Unit Cell (CCUC), Chulalongkorn University for very nice recommendation, will power and all their help.

Finally, I would like to thank Computational Chemistry Unit Cell (CCUC), Department of Chemistry, Faculty of science, Chulalongkorn University for computing resources and this work were supported by the National Research University Project of CHE and Ratchadaphiseksomphot Endowment Fund (HR1155A). The Center of Excellence for Petroleum, Petrochemicals and Advanced Materials, Chulalongkorn University is acknowledged.

I would not have achieved this far and this thesis would not have been completed without all the support that I have always received from there.

CONTENTS

	Page
ABSTRACT IN THAI.....	iv
ABSTRACT IN ENGLISH.....	v
ACKNOWLEDGMENTS.....	vi
CONTENTS.....	vii
LIST OF TABLES.....	ix
LIST OF FIGURES.....	x
LIST OF ABBREVIATIONS.....	xii
CHAPTER I Introduction.....	1
1.1 Key facts of cancer.....	1
1.1.1 Epidemiology of cancer.....	1
1.1.2 Causes of cancer.....	1
1.1.3 Cancer treatment.....	2
1.2 Cyclin Dependent kinases (CDKs).....	3
1.3 CDK6 path way	4
1.4 Literature reviews on CDK6.....	5
1.4.1 CDK6/Vcyclin structure.....	5
1.4.2 CDK6 inhibitors.....	6
1.5 Scope of this research work.....	9
CHAPTER II Theory.....	11
2.1 Molecular dynamics simulation.....	11
2.1.1 Statistical mechanics.....	11
2.1.2 Motion equation and classical mechanics.....	12
2.2 MM-PBSA calculation.....	13
2.3 Binding free energy decomposition.....	14
CHAPTER III Computational methods.....	16
3.1 System preparation.....	16
3.2 Force field parameters for inhibitors.....	17
3.3 Molecular dynamics simulations.....	17

CHAPTER IV Results and discussion	19
4.1 System stability.....	19
4.2 Kinase inhibitor binding pattern in active CDK6.....	20
4.2.1 Hydrogen interactions.....	20
4.2.2 Per residue inhibitor-enzyme interactions.....	22
4.2.3 Binding free energy (MM-PBSA).....	25
CHAPTER V Conclusions	27
REFERENCES	28
VITAE	32

LIST OF TABLES

	Page
Table 1.1 2D chemical structures and IC_{50} of each inhibitor.....	7
Table 1.2 2D chemical structure, IC_{50} and binding energy of each inhibitor.....	8
Table 4.1 The binding free energy (kcal/mol) and its components of the three kinase inhibitors (FST, AGN and CHS) in four complexes FST-CDK6/v, AGN-CDK6/v, CHS_A-CDK6/v and CHS_B-CDK6/v where the experimental IC_{50} values taken from ref. 10 were also given.....	25

LIST OF FIGURES

	Page
Figure 1.1 Epidemiology of cancer.....	1
Figure 1.2 The normal cell division versus the division of cancer cell.....	2
Figure 1.3 Four phases (G1, S, G2 and M) in the cell cycle controlled by CDK/cyclin complexes.....	4
Figure 1.4 Pathway of CDK6/Cyclin D complex activation for phosphorylation reaction.....	5
Figure 1.5 (a) The crystal structure of fisetin, FST, in the ATP binding site of the active CDK6 in complex with Vcyclin. (b) The hydrogen bonds formed between FST and the side chain and backbone of binding residues at the CDK6 binding site.....	6
Figure 1.6 Chemical structures of Cyclin Dependent Kinase (CDK) inhibitors, fisetin (FST), apigenin (AGN) and chrysin (CHS).....	10
Figure 2.1 Molecular dynamics simulation algorithm.....	13
Figure 3.1 The box simulation for CDK 6/Vcyclin complex with fisetin bound.	17
Figure 4.1 RMSD plots for the four systems studied: (a) FST-CDK6/v, (b) AGN-CDK6/v, (c) CHS_A-CDK6/v, and (d) CHS_B- CDK6/v.....	19
Figure 4.2 (I): Percent occupation of hydrogen bonds between the CDK6 residues and inhibitor at three moieties (A-C are identical to these defined in Figure 1.6) for the four systems studied here: (a) FST- CDK6/v, (b) AGN- CDK6/v, (c) CHS_A- CDK6/v, and (d) CHS_B- CDK6/v. (II): The schematic view of inhibitor-CDK6/v interactions taken from the last MD snapshot.....	20
Figure 4.3 Decomposition of the free energy on a per-residue basis of residues in the N-terminal domain, the hinge region and the C-terminal domain into the contributions from the atom groups of the backbone and side chain in the CDK6/Vcyclin complex bound to (a) FST, (b) AGN, (c) CHS_A and (d) CHS_B.....	22

Figure 4.4 Energy contribution of electrostatic ($E_{ele} + G_{polar}$) and van der Waals ($E_{vdW} + G_{nonpolar}$) terms for the residues in the N-terminal domain (violet), the hinge region (orange) and the C-terminal domain (green) of the CDK6/Vcyclin complexed with inhibitors. (a) FST-CDK6/v, (b) AGN-CDK6/v, (c) CHS_A-CDK6/v and (d) CHS_B-CDK6/v..... 23

LIST OF ABBREVIATIONS

2D	=	Two dimension
3D	=	Three dimension
ADP	=	Adenosine diphosphate
AGN	=	Apigenin
Ala(A)	=	Alanine
Asp(D)	=	Aspartic acid
ATP	=	Adenosine triphosphate
CDK6	=	Cyclin Dependent Kinase 6
CDK6/Vcyclin	=	Cyclin Dependent Kinase 6 complex with Vcyclin
CDKs	=	Cyclin Dependent Kinases
CHS	=	Chrysin
DC	=	Decomposition
DHFR	=	Dihydrofolate reductase
DNA	=	Deoxyribonucleic acid
EGCG	=	Epigallocatechol gallate
FST	=	Fisetin
Gln(Q)	=	Glutamine
Glu(E)	=	Glutamic acid
HF	=	Hartree-Fock
His(H)	=	Histidine
Ile(I)	=	Isoleucine
K	=	Kelvin
kcal	=	Kilocalorie
Leu(L)	=	Leucine
Lys(K)	=	Lysine
MD	=	Molecular Dynamics
Phe(F)	=	Phenylalanine
Rb	=	Retinoblastoma tumor suppressor gene product
RMSD	=	Root mean square deviation
RNA	=	Ribonucleic acid

TS	=	Thymidylate synthase
Val(V)	=	Valine
Vcyclin	=	Virus-encoded cyclin from herpesvirus saimiri
vdW	=	van der Waals
μM	=	Micromolar

CHAPTER I

INTRODUCTION

1.1 Key facts of cancer

1.1.1 Epidemiology

Cancer is a leading cause of death worldwide and accounts around 13% of all deaths (7.6 million deaths) in 2008 [1]. More than 70% of all cancer deaths occurred in low- and middle-income countries. The major types of cancer are lung (1.4 million deaths), stomach (740,000 deaths), liver (700,000 deaths), colorectal (610,000 deaths) and breast (460,000 deaths).

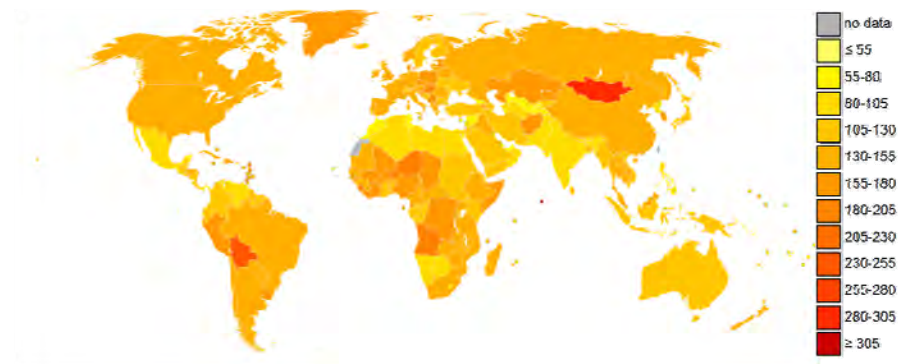


Figure 1.1 Epidemiology of cancer: death rate from malignant cancer per 100,000 inhabitants in 2004 [2].

1.1.2 Causes of cancer

Cancer is caused by either internal factors (such as inherited mutations, hormones, and immune conditions) or external factors (such as tobacco, diet, radiation, and infectious organisms) or both of them [3]. The cancer is a term used for diseases in which abnormal cells divide without control, uncontrolled cellular proliferation, restricted apoptosis, and angiogenesis [4].

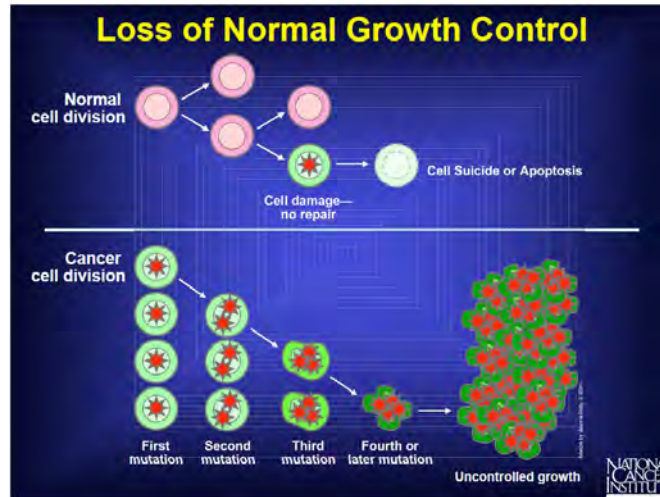


Figure 1.2 The normal cell division (top) versus the division of cancer cell (bottom) [5].

Cancer arises from a loss of normal growth control (Figure 1.2). In normal tissues, the rates of new cell growth and old cell death are kept in balance but in cancer this balance is interrupted. The disruption can result from uncontrolled cell division or loss of a cells ability to undergo cell suicided by a process called apoptosis, the mechanism by which old or damaged cells normally self-destruct.

1.1.3 Cancer treatment

A number of medical treatments are employed to cure cancer including, surgery, radiation therapy and chemotherapy. They depend on patient's condition. Nevertheless the chemotherapy is one of primary approach for general patients. Mechanistic action of anti-cancer agents can be considered into three main categories as follows [6].

1. *Stop the synthesis of DNA molecule:* The agents block some steps in the formation of nucleotides that is necessary for making DNA. When these steps are blocked, the cells cannot replicate because they cannot make DNA without the nucleotides. Examples of drugs in this class include methotrexate (Abitrexate®), fluorouracil (Adrucil®), hydroxyurea (Hydrea®), and mercaptopurine (Purinethol®).

2. *Directly damage the DNA:* The agents chemically damage DNA and RNA. They disrupt replication of the DNA or RNA. Examples of anti-cancer for this class are cisplatin (Platinol®), antibiotics - daunorubicin (Cerubidine®), doxorubicin (Adriamycin®), and etoposide (VePesid®).
3. *Effect the synthesis or breakdown of the mitotic spindles:* The mitotic spindles are very important because they help to split the newly copied DNA such that a copy goes to each of the two new cells during cell division. These drugs disrupt the formation of these spindles and therefore stop cell division. Drugs in this class are such as Vinblastine (Velban®), Vincristine (Oncovin®) and Paclitaxel (Taxol®).

There are many categories of commercial anti-cancer medicines activating to DNA replication or chromosome segregation aimed to stop cell division [7]. However, their negative side effects on the normal cell have been found. Thus the development of a high efficiency therapy with decreased toxicity is desirable. The cyclin dependent kinase is an interesting target to discover new pathway that remedies these problems.

1.2 Cyclin Dependent kinases (CDKs)

The cyclin dependent kinases (CDKs) are the groups of serine/threonine kinases and play direct role in cell cycle. They involve in the regulation of the cell cycle, neuronal function, transcription and apoptosis that cause of cancer. It becomes active only in association with a regulatory partner cyclin [8]. The cell cycle can be divided into four phases (Figure 1.3). The preparation of nutrition is done during the interphase containing three stages: G1, S, and G2. In mitosis (M phase), the cell divides into two daughter cells.

CDKs contain 13 family members [9-13], namely CDK1-CDK13. The role of CDKs is to drive the cell forward through next phase of the cell cycle until cell division. The pattern of cyclin expression defines the relative position of cell within the periods of the cell cycle [14, 15]. The association of cyclin D with CDK2, CDK4 and CDK6 drive the cell in G0 forward through to half of G1 phase. CDK2/Cyclin E complex functions in the S phase at G1/S transition. The CDK2/cyclin A is important to the DNA synthesis in S phase. Then, cell driving from G2 to M phase is activated

by CDK1/cyclin A. Finally, CDK1/cyclin A activates cell in G2 phase dividing into two daughter cells in M phase [16].

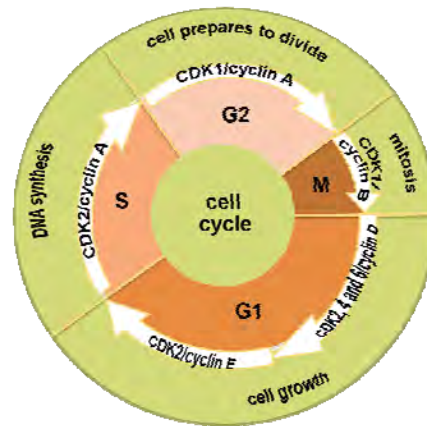


Figure 1.3 Four phases (G1, S, G2 and M) in the cell cycle controlled by CDK/cyclin complexes.

The CDK6 controls the entrance into the cell cycle. G0 drives G1 and can be crystallized. The CDK6 is a promising cancer target and have received a great research interest.

1.3 CDK6 path way

The cyclin dependent kinase 6 (CDK6) is one of protein kinases regulated by D-type cyclin and drives cell division by a phosphorylation reaction in the cell cycle [17]. Progression through the cell cycle is promoted by cyclin-dependent kinases (CDKs), which are regulated positively by cyclins and negatively by CDK inhibitors (CDKIs) (Figure 1.4).

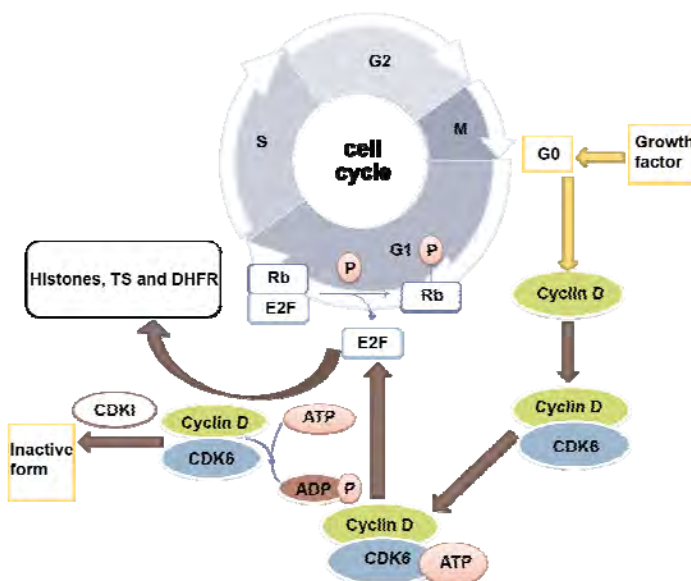


Figure 1.4 Pathway of CDK6/Cyclin D complex activation for phosphorylation reaction.

Healthy cells enter the cell cycle in G0 phase. The cells in G0 phase were stimulated by growth factors that signal of cell entry to the cell cycle. Mitogenic signaling of growth signals is mediated by the RAS/RAF/MAPK pathway, whose end point is the stimulation of D-type cyclin production [16]. The CDK6/cyclin D complex is activated by phosphorylation reaction at specific sites on the CDK by CDK-activating kinase (CAK), also referred to CDK7/cyclin H [17]. The CDK6/cyclin D complex extracts the phosphate group from adenosine 5'-triphosphate (ATP) at ATP-binding pocket where the ADP and independent phosphate group are found. The retinoblastoma tumor suppressor gene product (Rb) governs the G1/S transition. In active state, Rb is hypophosphorylated and forms an inhibitory complex with a group of transcription factors known as E2F, thus controlling the G1/S transition. When Rb is partially phosphorylated by CDK4/6-cyclin, E2F transcription factor is still able to transcribe some genes and over expression [18].

1.4 Literature reviews on CDK6

1.4.1 CDK6/Vcyclin structure

The X-ray structure of apo-form, human cyclin dependent kinase 6 (CDK6) preferentially forms complexes with cyclin from herpesvirus saimiri (Vcyclin). This

structure deposited in the protein data bank (PDB) entry code 1JOW, was first published in 2002 by Gahmen and kim [19]. The CDK6/Vcyclin apo-form provides the structural basis of CDK6 activation by viral cyclins. In 2005, Lu *et al.* [20] crystallized the CDK6/Vcyclin inhibited by fisetin or 3, 7, 3', 4'-tetrahydroxyflavone entry code 1XO2. CDK6 contains 2 domains, the N-terminal domain in β -sheet (residues 1-100) and the C-terminal with mostly α -helical (residues 101-308). The X-ray structure of CDK6/Vcyclin with fisetin bound shows that the inhibitor binds in the ATP-binding pocket of CDK6 (Figure 1.5a). The 3', 4'-dihydroxyphenyl group in B ring points into the binding pocket where the α -phosphate of ATP would bind (Figure 1.5a). The hydrogen bonds between FST and CDK6 detected are summarized in Figure 1.5b.

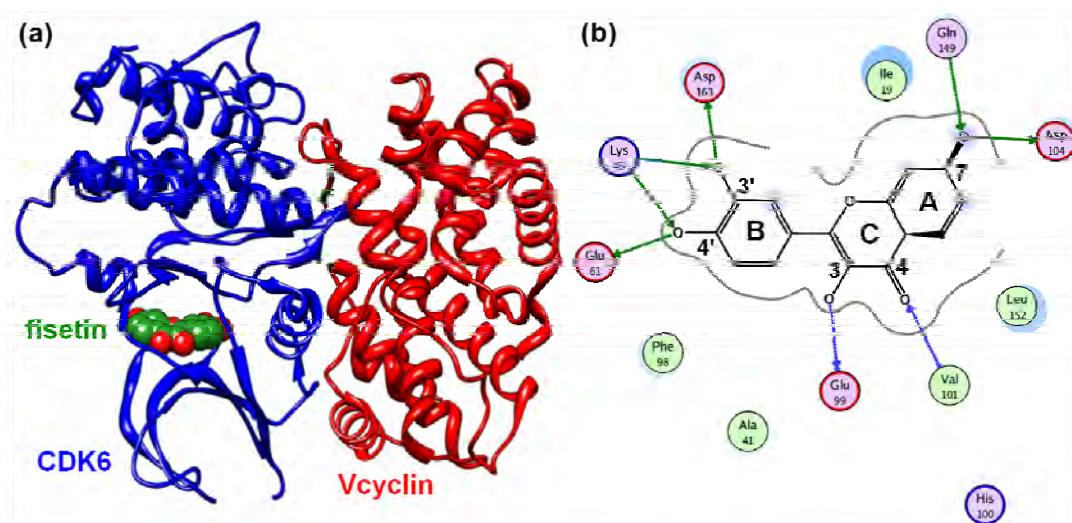
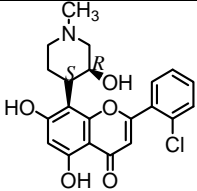
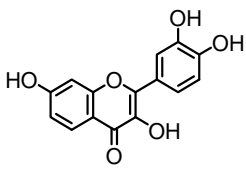
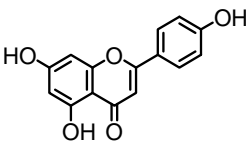
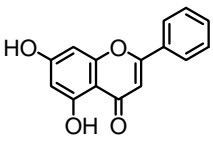
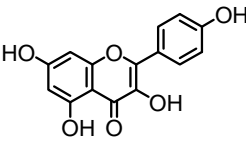
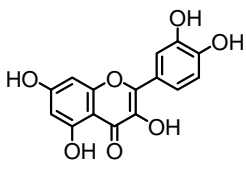
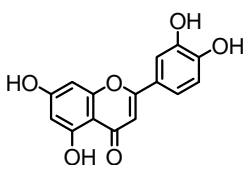


Figure 1.5 (a) The crystal structure of fisetin, FST, in the ATP binding site of the active CDK6 (blue) in complex with Vcyclin (red). (b) The hydrogen bonds formed between FST and the side chain and backbone of binding residues at the CDK6 binding site were shown by green and blue arrows.

1.4.2 CDK6 inhibitors

Currently, there are many categories of CDK6 inhibitors, including flavonoids. The IC_{50} values of the flavonoid compounds inhibiting CDK6/Vcyclin [20] were summarized in table 1.1.

Table 1.1 2D chemical structures and IC_{50} of each inhibitor

Inhibitor	Chemical structures	IC_{50} value (μM)
flavopiridol		0.08
fisetin		0.85
apigenin		1.70
chrysin		6.00
kaempferol		22.00
quercetin		25.00
luteolin		>300.00

The flavopiridol containing the 4-(3-hydroxy-1-methyl)-piperidinyl on benzopyran is different from the other inhibitors. It shows the highest inhibitory affinity toward CDK6/Vcyclin.

In 2010, Phosrithong and Ungwitayatorn [21] studied the binding mode and binding free energy of natural products inhibiting several cancer targets, including CDK6/Vcyclin, by the molecular docking method.

Table 1.2 2D chemical structure, IC_{50} and binding energy of each inhibitor

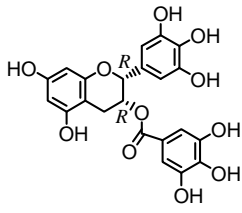
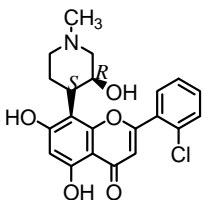
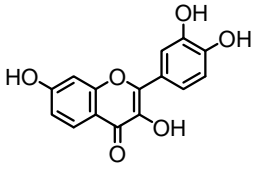
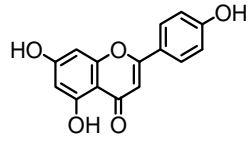
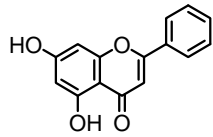
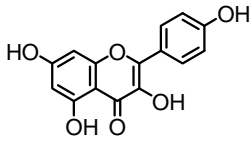
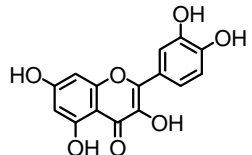
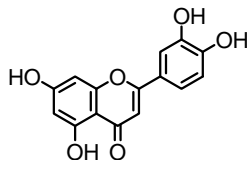
Inhibitor	Chemical structure	IC_{50} value (μ M)	Binding energy (kcal/mol)
EGCG		-	-12.70
flavopiridol		0.08	-11.20
Fisetin		0.85	-9.93
apigenin		1.70	-9.10
chrysin		6.00	-8.52

Table 1.2 2D chemical structure, IC_{50} and binding energy of each inhibitor (cont.).

Inhibitor	Chemical structure	IC_{50} value (μ M)	Binding energy (kcal/mole)
kaempferol		22.00	-9.45
quercetin		25.00	-9.85
luteolin		>300.00	-9.78

The EGCG, a natural product, had the lowest binding energy to the CDK6/Vcyclin complex; however, the calculated binding free energies are not in good agreement with the experimental IC_{50} value (Table 1.2). Zhang *et al.* used homology modeling, molecular docking and molecular dynamics simulations for study on the inhibition of CDK1 by flavopiridol [22].

1.5 Scope of this research work

To obtain the fundamental information of protein-drug interactions, molecular dynamics simulations of on the three flavonoid compounds, FST, AGN and CHS, binding to CDK6/Vcyclin at the ATP-binding pocket were performed. These studies aim to demonstrate the intermolecular interactions and binding free energy of three inhibitors, fisetin (FST), apigenin (AGN) and two-orientation of chrysin (CHS), in complex with the CDK6/Vcyclin. Note that the chosen three inhibitors under drug development process exhibit different numbers and positions of hydroxyl group substitution on the core structure. The FST and CHS are under *in vivo* study while that AGN is in the clinical trial Phase II [23]. Particular interactions between

CDK6/Vcyclin and inhibitor could be a helpful drug discovery and design of new potent anticancer agents.

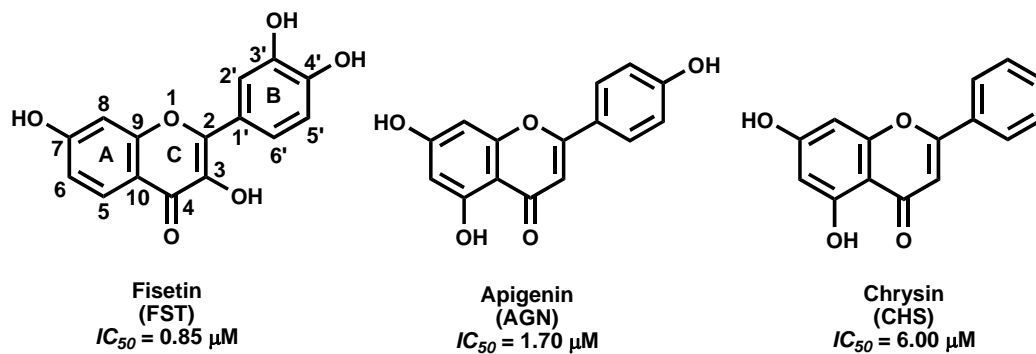


Figure 1.6 Chemical structures of Cyclin Dependent Kinase (CDK) inhibitors, fisetin (FST), apigenin (AGN) and chrysin (CHS).

CHAPTER II

THEORY

2.1 Molecular dynamics simulation

It has been 34 years since the report of the first molecular dynamics (MD) simulations of a protein was published [24]. Heretofore, these methods have become a confirmed method for study of macromolecule of biological, complementary to experimental techniques. The MD simulation defines to “a computer simulation technique where configuration or conformational space is explored on the basis of the time evolution by integrating their equation of motion” [25].

2.1.1 Statistical mechanics

MD simulations get information at the microscopic level, including atomic positions and velocities. The microscopic information (as governed by schrödinger’s equation or newton’s laws of motion) can convert to observed properties of a large system such conformational change, binding free energy and mechanism via statistical mechanics [26, 27]. Statistical mechanics is important to study of biological systems by molecular dynamics simulation. Molecular dynamics simulations construct a sequence of points in phase space as a function of time and collect points in phase space satisfying the conditions of macroscopic state celled ensemble. An ensemble is a collection of all possible systems which have different microscopic states but have an identical macroscopic state. In statistical mechanics, average values for observables are defined as ensemble averages and the time averages were calculated by MD simulation. That is one truth of statistical mechanics, the Ergodic hypothesis state according to Eq. 1.

$$\langle A \rangle_{ensemble} = \langle A \rangle_{time} \quad (1)$$

The hypothesis concept is the system will ultimately pass through all possible states when this system was allowed, to evolve in time indefinitely. The time of

simulations should be long enough obtaining the representative conformations that this equality is satisfied.

2.1.2 Motion equation and classical mechanics

A molecular dynamics simulation is the computational method that defines to the time-dependent behavior of the system by solving newton's laws (2nd law) of motion define in Eq. 2.

$$F_i = m_i a_i \quad (2)$$

where F_i is the force which interacted on the atom (i) at time (t), m_i is the mass of atom i and a_i is acceleration of atom i . The force can define in derivative from of potential function (V) according in Eq. 3 and a can transform into 1st derivative and 2nd derivative of velocity and position, respectively.

$$F_i = -\nabla_i V = m_i a_i = m_i \frac{dv}{dt} = m_i \frac{d^2x}{dt^2} \quad (3)$$

From integration of velocity can define equation between the positions, velocities, accelerations and time as Eq. 4.

$$x_i = a_i t^2 + v_0 t + x_0 \quad (4)$$

The initial atom position, an initial distribution of velocities and the acceleration, is determined base on potential function (V), is a summation between bonded and non-bonded interactions. The bonded interaction term can divided into bond, angle and dihedral energy. To calculate the new coordinate and velocity of atom at all other times, can determine by this equation (Eq. 4), starting at time zero. The simulation proceeds define by calculating forces and solving the equations of motion based on the

accelerations obtained from the new forces. Generally, MD process can be divided into two steps: predictor and corrector in solving the equations of motion according to Figure 2.1.

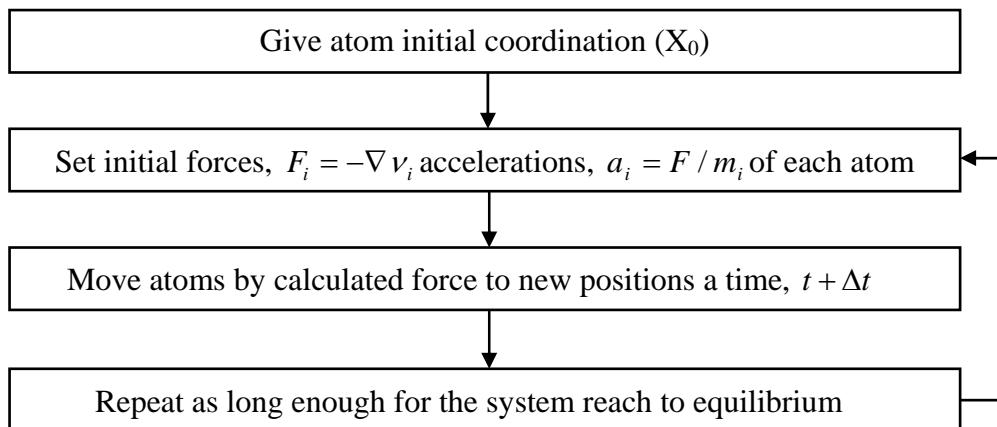


Figure 2.1 Molecular dynamics simulation algorithm

To check the equilibrium of the system, we monitored the root mean square deviation (RMSD) and the stability of the energy. The results were taken from the MD trajectory, and the properties of the system were calculated from these.

2.2 MM-PBSA calculation

The MM-PBSA is an acceptable method in the Amber package to evaluate the free energies of binding or to estimate the absolute free energies of molecules in solution. The binding free energy of the system was obtained from the difference of the free energies between the complex (ΔG_{cpx}), protein (ΔG_{prot}) and ligand (ΔG_{lig}):

$$\Delta G_{bind} = \Delta G_{cpx} - [\Delta G_{prot} + \Delta G_{lig}] \quad (5).$$

In general, the total free energy is computed from the enthalpy term (ΔH) and the entropic contribution at a constant temperature ($T\Delta S$),

$$\Delta G = \Delta H - T\Delta S \quad (6).$$

The ΔH term of the system was obtained from the summation of enthalpy changes in the gas phase upon complex formation (ΔE_{MM}) and the solvated free energy contribution (ΔG_{sol}). Therefore, Eq. 6 can be approximated as:

$$\Delta G = (\Delta E_{MM} + \Delta G_{sol}) - T\Delta S \quad (7)$$

where ΔE_{MM} corresponds to the molecular mechanical energy, including the bonded and nonbonded energy terms. The latter one is composed of the electrostatic (ΔE^{ele}) and vdW (ΔE^{vdw}) interaction energies. ΔG_{sol} accounts for the solvation energy which is divided into the electrostatic component (ΔG_{sol}^{ele}) and a nonpolar component ($\Delta G_{sol}^{nonpolar}$),

$$\Delta G_{sol} = \Delta G_{sol}^{ele} + \Delta G_{sol}^{nonpolar} \quad (8).$$

The Poisson-Boltzmann (PB) method was used to compute the electrostatic component while the nonpolar term in solvation free energy was evaluated according to Eq. 9.

$$\Delta G_{sol}^{nonpolar} = \gamma SASA + \beta \quad (9),$$

where SASA is the solvent accessible surface area (\AA^2) of each given molecule. The solvent probe radius is of 1.4 \AA , and the experimental solvation parameters, γ and β , are 0.0072 kcal/mol \AA^2 and 0.00 kcal/mol, respectively.

In this present work, the MM/PBSA binding free energy calculation was performed using the MM/PBSA module in Amber 10 where the CDK6/Vcyclin is considered as protein and the three different ligands are FST, AGN, CHS_A and CHS_B. Since the systems of all flavonoid compounds binding to the same CDK6/Vcyclin, it can be assumed that the difference in entropy contribution should be rather small. Thus, the entropy part can be omitted from the binding free energy calculation as justified in some previous studies [28, 29].

2.3 Binding free energy decomposition

The contribution of each residue in CDK6/Vcyclin to the free energy of protein-ligand binding in Eq. 5 is evaluated by the free energy decomposition. The Generalized Born (GB) model was used to calculate electrostatic contribution to the solvation as expressed in Eq. 10,

$$\Delta G_{sol}^{ele} = -\frac{1}{2} \left(1 - \frac{e^{-\kappa r}}{\epsilon_{\omega}} \right) \sum_{ij} \frac{q_i q_j}{f_{GB}} \quad (10).$$

The Debye-Hückel screening parameter, κ , and solvent dielectric constant, ϵ_{ω} , were set to 0 and 80, respectively. f_{GB} was obtained by:

$$f_{GB} = \left[r_{ij}^2 + \alpha_i \alpha_j \exp\left(\frac{-r_{ij}^2}{4\alpha_i \alpha_j}\right) \right]^{\frac{1}{2}} \quad (11)$$

where α_i and α_j are the effective Born radius of atoms i and j , while r_{ij} is the distance between these two atoms. The contribution of atom i to the electrostatic free energy is evaluated by Eq. 12.

$$\Delta G_{sol}^{ele}(i) = -\frac{1}{2} \sum_j \left(1 - \frac{e^{-\kappa r}}{\epsilon_\omega} \right) \frac{q_i q_j}{f_{GB_{ij}}(r_{ij})} + \frac{1}{2} \sum_{j \neq i} \frac{q_i q_j}{r_{ij}} \quad (12)$$

The nonpolar solvation energy per atom was approximated according the SASA as given by Eq. 13.

$$\Delta G_{nonpolar,sol}^i = \gamma \times (SASA^{i,cpx} - (SASA^{i,prot} + SASA^{i,lig})) \quad (13)$$

where $SASA_{i,prot}$ or $SASA_{i,lig}$ is equal to zero depending on which component the atom belongs to. In addition, the total electrostatic interaction energy between two components (ΔE_{ele}^i) was obtained by one haft of pairwise electrostatic interaction energy between the two atoms. Likewise the pairwise van der Waals interaction energy (ΔE_{vdw}^i) between protein and ligand was assigned to avoid double counting. The calculation of the internal energy and entropy terms is equal to zero under the assumption of a single trajectory approach because the energies of the complex and the separated parts are calculated from the same trajectory. Therefore, the contribution of binding free energy for a per-residue basis can be evaluated from the summation of the atomic contributions, (ΔE_{ele}^i), (ΔE_{vdw}^i), ΔG_{sol}^{ele} and $\Delta G_{sol}^{nonpolar}$, over the atoms of a given residue without entropy term.

CHAPTER III

COMPUTATIONAL METHODS

3.1 System preparation

The four simulated systems of CDK6/Vcyclin complexed with the three inhibitors FST, AGN, and CHS were prepared, in which the third inhibitor was oriented in two binding conformations. The initial structure of FST-CDK6/v complex was taken from the Protein Data Bank (PDB), entry code 1XO2. To construct the initial structure of the other two inhibitors, the atomic coordinates of the FST in the FST-CDK6/v were separately modified to get the AGN-CDK6/v and CHS_A-CDK6/v complexes. For the CHS in the deschloro-flavopiridol-like orientation (CHS_B) binding to the CDK6/Vcyclin, the CHS_B-CDK6/v structure was obtained by docking procedure using the CDOCKER module in the Discovery Studio 2.5

The starting structure preparation and MD simulations were performed using Amber 10 software package [30] with ff03 force field [31]. The LEaP module was used to correct all missing hydrogen atoms of the protein and ligand. The ionizable side chains of amino acids, Lys, Arg, Asp and Glu, were defined at *pH* 7.0. For His residues, exclude the di-protonated His73 and His297, a neutral charge with mono-protonation on the δ -nitrogen atom was given to all the rest. To reduce bad steric interactions, the hydrogen atoms were only minimized with 1000 steps of steepest descents (SD), continued by 500 steps of conjugated gradient (CG). Then, each system was solvated by TIP3P waters [32] with the minimum distance of 10 Å from the protein surface. As a result, the water box size of all systems was 98 x 88 x 83 Å³, while the total atoms were 59108, 59107, 59106 and 59109 for the FST-, AGN-, CHS_A- and CHS_B-CDK6/v complexes, respectively. A total charge of -3 was achieved for all systems and was consequently neutralized by adding 3 Na⁺ ions. The SD (2000 steps) and CG (1000 steps) minimizations were carried out on the water molecules alone and subsequently on the whole system with the same minimized procedure to obtain the starting structures for MD simulation in the next step.

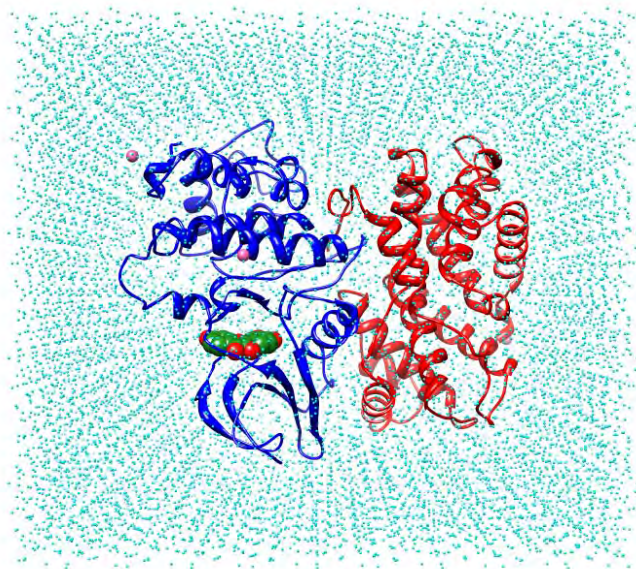


Figure 3.1 the box simulation for CDK 6/Vcyclin complex with fisetin bound.

3.2 Force field parameters for the inhibitors

The empirical force field parameters of the three inhibitors were developed according to the standard procedure [29, 33 and 34]. The hydrogen atoms were added to the inhibitor atomic coordinates by consideration on the hybridization of the covalent bonds. Using Gaussian 03 program [35], the structure optimization with the HF/6-31* basic set was performed to adjust bond lengths and bond angles of ligand. The optimized geometry was, then, used to calculate the HF/6-31G* electrostatic potential (ESP) surrounding the inhibitor molecule. The RESP charges were finally obtained by charge-fitting procedure with the RESP module of Amber. The missing bonded parameters for inhibitor were gained from the Generalized Amber Force Field (GAFF) [36], while the standard van der Waals parameters were used to sufficient transferability of inter-molecules.

3.3 Molecular dynamics simulations

The MD simulations were performed using SANDER module in Amber and the periodic boundary with NPT ensemble at 1 atm was applied. The SHAKE algorithm [37] was used to constrain all bonds involving hydrogen atoms and the time step of 2 fs and was used. The distance cutoff function for nonbonded interactions was set at 12 Å and the

particle mesh Ewald method [38] was applied for an adequate treatment of long-range electrostatic interactions. The whole system was heated up to 298 K for 60 ps and subsequently simulated at 298 K for equilibration and production phases. All systems were well equilibrated at 6 ns. Therefore, the simulations were prolonged for another 4 ns in all systems. The MD trajectories were extracted from the production phases, the last 4 ns, for analysis.

The stability of the system was monitored through the convergences of energy, temperature, and global root mean-square displacement (RMSD). The ptraj and MM-PBSA modules were used to analyze the root mean square deviation (RMSD), hydrogen bond between inhibitor and protein, decomposition of free energies per residue ($\Delta G_{bind}^{residue}$) and binding free energies (ΔG_{bind}) as well as their energy components.

CHAPTER IV

RESULTS AND DISCUSSION

4.1 System stability

The stability of the four systems was determined by the RMSD of the MD trajectories obtained from simulations with respect to initial structure. The results were plotted and compared in Figure 4.1. RMSDs for overall atoms, backbone atoms of CDK6 and Vcyclin, inhibitors, and backbone atoms of the residues within a 7 Å sphere of inhibitor were given separately.

In all systems, the RMSD of CDK6 backbone atoms (blue in Figure 4.1, see also Figure 1.5 for 3D structure) are relatively higher than that of Vcyclin backbone atoms (red). While the RMSD fluctuations demonstrated the flexibility of the two proteins, the RMSD plots for inhibitor (green) and the backbone atoms of its binding residues (pink) tended to be steady along the simulation time. Taken altogether with the RMSD for overall atoms (black), all complexes were likely to reach equilibrium at 6 ns. This is therefore the MD trajectories from the last 4 ns simulation of all systems were taken for analysis.

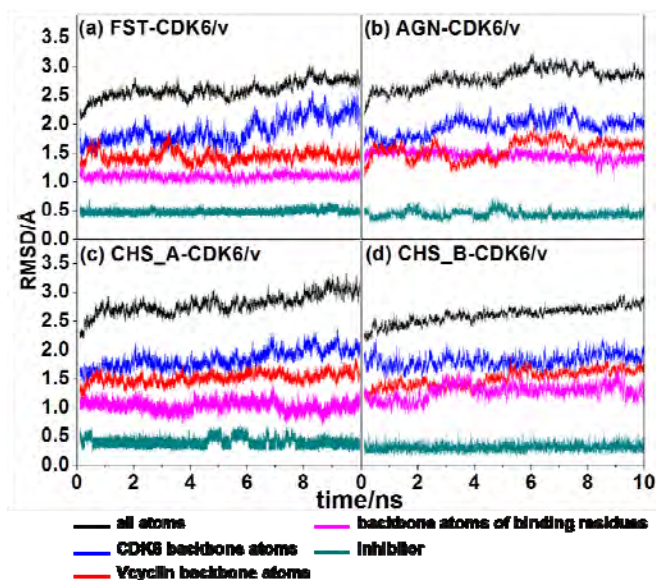


Figure 4.1 RMSD plots for the four systems studied: (a) FST-CDK6/v, (b) AGN-CDK6/v, (c) CHS_A-CDK6/v, and (d) CHS_B-CDK6/v.

4.2 Kinase inhibitor binding pattern in active CDK6

4.2.1 Hydrogen interactions

All inhibitors studied here are classified as flavonoids, containing different numbers of hydroxyl group substitutions on the three rings, A-C as shown in Figure 1.6. Hydrogen bonding between these hydroxyl groups as well as the carbonyl oxygen of these flavonoids and the surrounding residues is an important factor in inhibitor binding at the active site. To monitor such interaction, the percentage and number of hydrogen bonds were calculated according to the following criteria: (i) proton donor-acceptor distance ≤ 3.5 Å; and (ii) donor-H-acceptor bond angle $\geq 120^\circ$. The results were shown in Figure 4.2, where the strong and medium hydrogen bond interactions are defined from the H-bond occupations of higher than 75% and 50%, respectively.

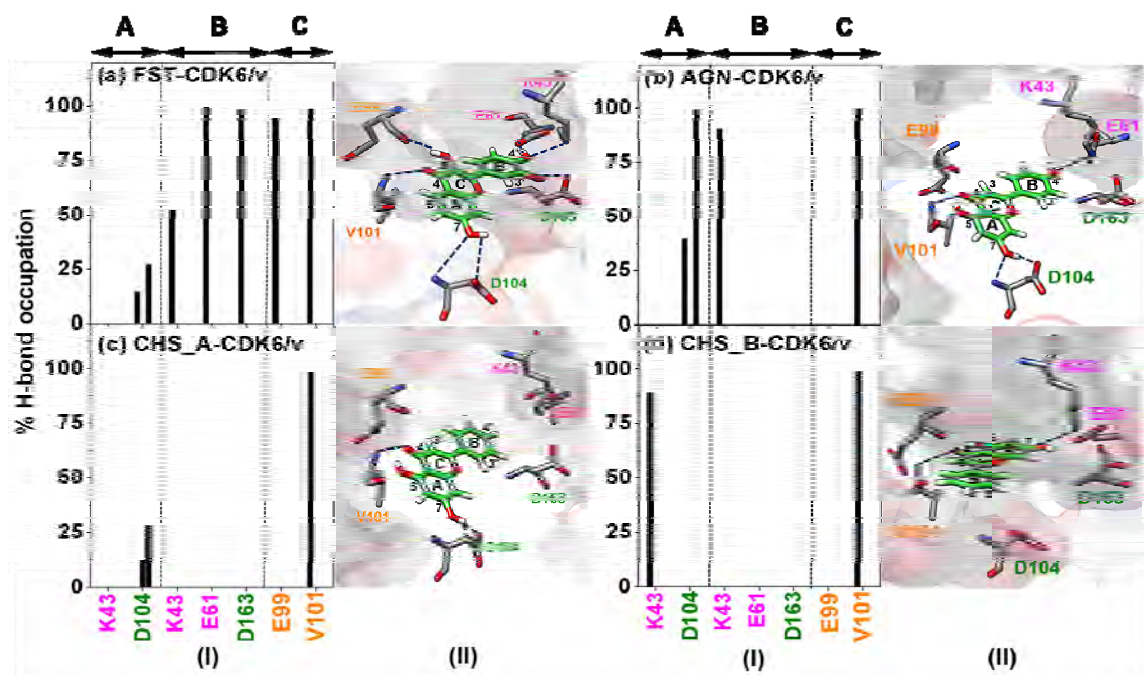


Figure 4.2 (I): Percent occupation of hydrogen bonds between the CDK6 residues and inhibitor at three moieties (A-C are identical to these defined in Figure 1.6) for the four systems studied here: (a) FST-CDK6/v, (b) AGN-CDK6/v, (c) CHS_A-CDK6/v, and (d) CHS_B-CDK6/v. (II): The schematic view of inhibitor-CDK6/v interactions taken from the last MD snapshot.

Figure 4.2 ligand-enzyme interactions in the three complexes are in the following order: FST-CDK6/v > AGN-CDK6/v > CHS_A-CDK6/v ~ CHS_B-CDK6/v. The total number of the H-bond interactions formed between inhibitor and the binding residues are 7, 4, 3 and 2 for the FST-CDK6/v, AGN-CDK6/v, CHS_A-CDK6/v and CHS_B-CDK6/v, with the number of strong hydrogen bonds of 4, 3, 1 and 2, respectively. The conserve H-bonds were formed at A- and C-ring (see Figure 1.6 for definition) of the inhibitor. In the A-ring, the two H-bond at the 7-OH group with the $-\text{COO}^-$ group and the N atom of the D104, the binding residue in the C-terminal domain, were detected in all systems with the FST-like form (Figure 4.2a-4.2c) with variation in % occupation. The other weak H-bond found in FST and AGN. This is not include the CHS_B-CDK6/v in which the ligand conformation is different from that of CHS_A-CDK6/v (see in Figure 4.2) and, hence the H-bond was found to form with the positively charge residue, K43 indeed. The other conserved strong H-bond at the C-ring was found between the 4-keto group of the three inhibitors and the backbone nitrogen of V101 as shown in Figure 4.2a-4.2d.

The other set of H-bond which supposed to play role in increasing sucessibility of the inhibitor, depends on number and position of the $-\text{OH}$ group in the A-, B- and C-ring. In A-ring, addition of the $-\text{OH}$ group at 5-position in AGN and CHS inhibitors has no effect in inhibitor binding at the CDK active site, *i.e.*, no more H-bond was found in Figure 4.2b-4.2c relative to those in Figure 4.2a. In addition, the presence of the 3-OH group in the C-ring in the FST has induced one more H-bond strongly formed with the backbone carbonyl oxygen of E99 (Figure 4.2a). Formation of this H-bond, in addition to that interesting to the V101 which available for all three inhibitors, make the FST oriented and anchored well in the hinge region between the N- and C-terminal domains of protein kinase as in consistent with those found in the X-ray structure (Figure 1.5b).

For the dihydroxylphenyl ring of FST (B-ring in Figure 4.2a), the main stabilization to the 3'- and 4'-OH groups was accordingly contributed from the $-\text{COO}^-$ group of residues D163 and E61 in the C- and N-terminal domains, respectively, with almost 100 % occupation. In addition, the $-\text{NH}_3^+$ moiety of K43, the residue in the N-terminal domain, moderately interacted with the 4'-OH group of this compound. This is somewhat different to the X-ray structure of FST-CDK6/v complex where the K43 side

chain was found to stabilize both –OH groups (Figure 1.5b). In Figure 4.2b, the B-ring without the –OH group at 3'-position in AGN has significantly caused a reduction in H-bond interactions, *i.e.*, only a strong hydrogen bond was established from the 4'-OH group to the –NH₃ group of K43. As expected, there is no H-bond formation to the highly hydrophobic phenyl ring of CHS in both orientations (Figure 4.2c-4.2d). It is a worth to note that the important interactions with three catalytic residues of protein kinase, K43, E61 and D163, were only maintained in the FST-CDK6/v simulation

4.2.2 Per residue inhibitor-enzyme interactions

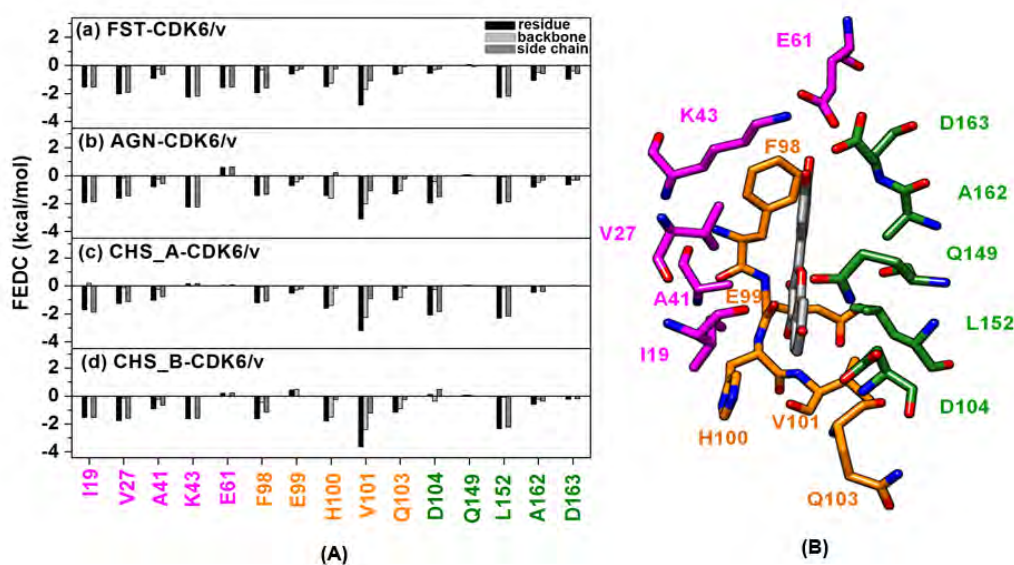


Figure 4.3 Decomposition of the free energy on a per-residue basis ($\Delta G_{bind}^{residue}$) of residues in the N-terminal domain (violet), the hinge region (orange) and the C-terminal domain (green) into the contributions from the atom groups of the backbone (light gray) and side chain (gray) in the CDK6/Vcyclin complex bound to (a) FST, (b) AGN, (c) CHS_A and (d) CHS_B

To explore the key binding motif of the flavonoid compounds inhibiting the CDK6/Vcyclin complex, the fundamental information of intermolecular interactions contributed from the residues contacted to each inhibitor were determined in leans of the pair interaction decomposition of free energy ($\Delta G_{bind}^{residue}$, the per residue total binding free

energy). In addition, contribution from the backbone atoms ($\Delta G_{bind}^{backbone}$) and the side chain atoms ($\Delta G_{bind}^{sidechain}$) were calculated separately. The 15 residues in the N-terminal domain, the hinge region and the C-terminal domain, were chosen according to the X-ray structure of the CDK6/Vcyclin with the FST bound [20]. The calculation was performed over the last 4-ns MD snapshots using the decomposition energy module in AMBER. The $\Delta G_{bind}^{residue}$ together with the $\Delta G_{bind}^{backbone}$ and the $\Delta G_{bind}^{sidechain}$ were summarized in Figure 4.3A. Moreover, the electrostatic ($E_{ele} + G_{polar}$) and van der Waals ($E_{vdW} + G_{nonpolar}$) energy terms of each residue were also evaluated and compared in Figure 4.4.

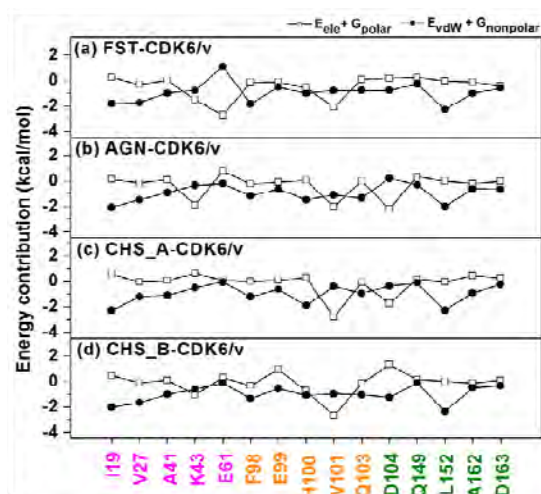


Figure 4.4 Energy contribution of electrostatic ($E_{ele} + G_{polar}$) and van der Waals ($E_{vdW} + G_{nonpolar}$) terms for the residues in the N-terminal domain (violet), the hinge region (orange) and the C-terminal domain (green) of the CDK6/Vcyclin complexed with inhibitors. (a) FST-CDK6/v, (b) AGN-CDK6/v, (c) CHS_A-CDK6/v and (d) CHS_B-CDK6/v.

It can be seen in Figure 4.3 that almost all inhibitor contacted residues provided the stabilization through their side chains, the $\Delta G_{bind}^{residue}$ (black) is almost contributed from the $\Delta G_{bind}^{sidechain}$ (dark gray). This is except for the four residues, 99-101 and 103, in the hinge region where the $\Delta G_{bind}^{backbone}$ (light gray) play stronger role to the $\Delta G_{bind}^{residue}$. In the N-terminal domain, the hydrophobic side chains of I19, V27 and A41 created the

favorable van der Waals contacts with the inhibitor molecule (dark gray in Figure 4.3 and vdW component in Figure 4.4), while the positively and negatively charged side chains of K43 (for FST-CDK6/v, AGN-CDK6/v and CHS_B-CDK6/v systems) and E61 (for the FST-CDK6/v) stabilized the inhibitor by providing electrostatic contribution (dark gray in Figure 4.3 and electrostatic component in Figure 4.4) via hydrogen bond formation. The residue V101 in the hinge region provided the highest degree of stabilization ($\Delta G_{bind}^{residue} \leq -3$ kcal/mol, black in Figure 4.3) among 15 residues to all inhibitors through its backbone ($\Delta G_{bind}^{backbone} \leq -2$ kcal/mol, light gray in Figure 4.3) forming a strong hydrogen bond with the inhibitor keto group as mentioned previously. This is supported by the energy contribution of this residue primarily from the electrostatic term of ≤ -2 kcal/mol (Figure 4.4). In contrast, the other four residues in this region partially built up the hydrophobic pocket for inhibitor as seen by more stabilizing vdW contributions in Figure 4.4. In the C-terminal domain, the L152 stabilization of -2 kcal/mol was found in all systems (black in Figure 4.3) mainly contributed from its hydrophobic side chain favorable vdW interacting to the benzopyran ring of inhibitor. The electrostatic stabilization from D104 was dominantly observed in the AGN-CDK6/v and CHS_A-CDK6/v systems (Figures 4.3 and 4.4) due to the firmly formed hydrogen bond and two weak H-bonds with the $-\text{COO}^-$ group, respectively (Figure 4.2).

In summary, the order of per-residue energy contribution from the surrounding residues to inhibitor was FST-CDK6/v > AGN-CDK6/v > CHR_A-CDK6/v ~ CHS_B-CDK6/v. The stabilizations were achieved from both electrostatic (hydrogen bond) and vdW components from these surrounding residues as described above.

4.2.3 Binding free energy (MM-PBSA)

The MM-PBSA free energy calculation was performed for all systems using the same set of snapshots as these used to evaluate the per-residue energy decomposition. The binding free energy (ΔG_{bind}) and the details of energy contributions are given in Table 4.1.

In gas phase (MM interaction energy), the order of the preferential favorable ΔE_{ele} contribution was FST-CDK6/v > AGN-CDK6/v > CHS_A-CDK6/v ~ CHS_B-

CDK6/v in which the corresponding ΔE_{ele} are $-53.0 < -46.9 < -30.4 < -28.0$ kcal/mol, respectively. This is in consistent with the order of number and percentage of hydrogen bond formations wanted earlier as well as the non-polar ($\Delta G_{sol}^{ele} + \Delta E_{ele}$) energy term, while the ΔE_{vdW} contribution was favorably found with similar amount for all systems (c.a. -33 to -36 kcal/mol). In contrast, the solvation free energy, the polar ($\Delta G_{sol}^{ele} + \Delta E_{ele}$) energy become unfavorable that is the values of 8.4, 12.6, 14.7 and 14.4 kcal/mol lead to the following order FST-CDK6/v < AGN-CDK6/v < CHS_A-CDK6/v < CHS_B-CDK6/v, respectively. This is due to the large extent determined by desolvation energy. This phenomenon has been also observed in some biological systems in solution [28, 39 and 40].

Taking into account the overall summation of the energy component, the binding free energies (ΔG_{bind}) of -30.5, -27.8, -23.3 and -26.1 kcal/mol were obtained for the FST-CDK6/v, AGN-CDK6/v, CHS_A-CDK6/v and CHS_B-CDK6/v, respectively. As shown in Table 4.1, the order of predicted binding efficiencies is in the same order as of the experimental inhibitory affinities, IC_{50} . Moreover, the ΔG_{bind} results in Table 4.1 suggest us also to conclude that the CHS in B orientation is better fits and binds into the ATP binding site of active the CDK6 than that in the orientation A (see in Figure 4.2 for definition). This is in consistent with the X-ray structure of the related analog, deschloro-flavopiridol, inhibiting the CDK2.

Table 4.1 The binding free energy (kcal/mol) and its components of the three kinase inhibitors (FST, AGN and CHS) in four complexes FST-CDK6/v, AGN-CDK6/v, CHS_A-CDK6/v and CHS_B-CDK6/v where the experimental IC_{50} values taken from ref. 10 were also given.

	FST-CDK6/v	AGN-CDK6/v	CHS_A-CDK6/v	CHS_B-CDK6/v
ΔE_{ele}	-53.0±8.6	-46.9±6.4	-30.4±4.4	-28.0±3.2
ΔE_{vdW}	-34.2±3.2	-35.7±3.3	-33.4±2.1	-36.0±2.5
ΔE_{MM}	-87.1±7.9	-82.6±5.6	-63.8±3.5	-64.0±3.8

Table 4.1 The binding free energy (kcal/mol) and its components of the three kinase inhibitors (FST, AGN and CHS) in four complexes FST-CDK6/v, AGN-CDK6/v, CHS_A-CDK6/v and CHS_B-CDK6/v where the experimental IC_{50} values taken from ref. 10 were also given (cont.).

	FST-CDK6/v	AGN-CDK6/v	CHS_A-CDK6/v	CHS_B-CDK6/v
$\Delta G_{sol}^{nonpolar}$	-4.8±0.1	-4.6±0.4	-4.6±0.3	-4.5±0.1
ΔG_{sol}^{ele}	61.4±7.2	59.5±4.6	45.1±3.7	42.4±3.4
ΔG_{sol}	56.6±7.2	54.9±4.7	40.5±3.6	37.9±3.4
$\Delta G_{sol}^{ele} + \Delta E_{ele}$	8.4±5.0	12.6±5.1	14.7±3.5	14.4±3.7
$\Delta G_{sol}^{nonpolar} + \Delta E_{vdW}$	-39.0±1.7	-40.4±1.85	-38.0±1.2	-40.5±1.3
ΔG_{bind}	-30.5±4.5	-27.8±3.5	-23.3±2.9	-26.1±3.2
IC_{50} (μ M)	0.85	1.70		6.00

CHAPTER V

CONCLUSIONS

In this study, the molecular dynamics simulations were applied to seek the detailed information on the key intermolecular interactions and dynamic properties of the three flavonoid inhibitors FST, AGN and CHS binding to the CDK6/Vcyclin complex. Both electrostatic, especially through hydrogen bond formation, and vdW interactions are important factors in binding efficiency of flavonoids against the CDK6/Vcyclin. The inhibitor binding strength likely depends on the number and position of hydroxyl group substitutions as well as the inhibitor orientation in the ATP binding pocket. The interaction of carbonyl group of inhibitor with V101 is considerably conserved in all flavonoids with either A or B binding conformations, while the 3'- and 4'-OH groups on the B ring are found to significantly increase in binding and inhibitory efficiency. Based on MM/PBSA method, the order of the predicted inhibitory affinities of these three inhibitors toward the active CDK6 displayed in the same trend of the order of the experimental IC_{50} values, *i.e.*, FST > AGN > CHS. In addition, the CHS preferentially binds to the active CDK6 in the different orientation to FST and AGN but similar to its related analog, deschloro-flavopiridol, which was previously found in the CDK2 crystal structure. The obtained results are useful as the basic information for the further design of potent anticancer drugs specifically targeting at the CDK6 enzyme.

REFERENCES

- [1] World health organization. GLOBOCAN 2008 [online]. 2011. Available from: <http://globocan.iarc.fr/factsheets/populations/factsheet.asp?uno=900> [2011, March 17]
- [2] World health organization. WHO Disease and injury country estimates [online]. 2009. Available from: http://www.who.int/healthinfo/global_burden_disease/estimates_country/en/index.html [2011, March 9]
- [3] Anand, P., and others. Cancer is a preventable disease that requires major lifestyle changes. Pharm. Res. 25 (2008): 2097–2116.
- [4] Meyers, R.A. Cancer: from mechanisms to therapeutic approaches. weinheim: Wiley-VCH, 2007.
- [5] International cancer institute. What is cancer? [online]. 2010. Available from: <http://www.cancer.gov/cancertopics/cancerlibrary/what-is-cancer> [2011, March 3]
- [6] Ophardt C.E. Anti-cancer drug I [online]. 2003. Available from: <http://www.elmhurst.edu/~chm/vchembook/655cancer.html> [2011, March 1]
- [7] Krakoff, I.H. Cancer chemotherapeutic agents. CA-cancer. J. Clin. 27 (1977): 130-143.
- [8] Harper, J.W., and Adams, P.D. Cyclin-Dependent Kinases. Chem. Rev. 101 (2001): 2511–2526.
- [9] Morgan, D.O. Cyclin-dependent kinases: engines, clocks, and microprocessors. Annu. Rev. Cell. Dev. Bi. 13 (1997): 261–291.

- [10] Jeffrey, P.D., and others. Mechanism of CDK activation revealed by the structure of a cyclinA-CDK2 complex. Nature. 376 (1995): 313–320.
- [11] Dunphy, W.G. The decision to enter mitosis. Trends. Cell. Biol. 4 (1994): 202–207.
- [12] Hoffman, I., and Karsenti, E. The role of cdc25 in checkpoints and feedback controls in the eukaryotic cell cycle. J. Cell. Sci. 18 (1994): 75–79.
- [13] Hochegger, H., Takeda, S., and Hunt, T. Cyclin-dependent kinases and cell-cycle transitions: does one fit all?. Nat. Rev. Mol. Cell. Bio. 9 (2008): 910-916.
- [14] Grana, X., and Reddy, E.P. Cell cycle control in mammalian cells: Role of cyclins, cyclin dependent kinases (CDKs), growth suppressor genes and cyclin-dependent kinase inhibitors (CKIs). Oncogene 11 (1995): 211-219.
- [15] Johnson, D.G., and Walker, C.L. Cyclins and cell cycle checkpoints. Annu. Rev. Pharmacol. Toxicol. 39 (1999): 295-312.
- [16] Schwartz, G.K., and Shah, M.A. Targeting the cell cycle: A new approach to cancer therapy. J. Clin. Oncol. 23 (2005): 9408-9421.
- [17] Garrett, M.D. Cell cycle control and cancer. Curr. Sci. India. 81 (2001): 515-522.
- [18] Kaldis, P., Russo, A.A., Chou, H.S., Pavletich, N.P., and Solomon, M.J. Human and yeast cdk-activating kinases (CAKs) display distinct substrate specificities. Mol. Biol. Cell. 9 (1998): 2545-2560.
- [19] Schulze-Gahmen, U., and Kim, S.H. Structural basis for CDK6 activation by a virus-encoded cyclin. Nat. Struct. Biol. 9 (2002): 177-181.
- [20] Lu, H., Chang, D.J., Baratte, B., Meijer, L., and Schulze-Gahmen, U. Crystal structure of a human cyclin-dependent kinase 6 complex with a flavonol inhibitor, fisetin. J. Med. Chem. 48 (2005): 737-743.
- [21] Phosrithong, N., and Ungwitayatorn, J. Molecular docking study on anticancer activity of plant-derived natural products. Med. Chem. Res. 19 (2010): 817-835.
- [22] Zhang, L., Zhu, H., Wang, Q., Fang, H., Xu, W., and Li, M. Homology modeling, molecular dynamic simulation and docking studies of cyclin dependent kinase 1. J. Mol. Model. 17 (2010): 219–226.
- [23] National Institutes of Health. Search for Clinical Trials [online]. 2008. Available from: <http://clinicaltrials.gov> [2011, March 2]

- [24] McCammon, J.A., Gelin, B.R., and Karplus, M. Dynamics of folded proteins. Nature. 267 (1977): 585-590.
- [25] Allen, M.P. Introduction to molecular dynamics simulation. NIC. Series. 23 (2004): 1-28.
- [26] McQuarrie, D.A. Statistical Mechanics. New York: Harper & Row, 1976.
- [27] Chandler, D. Introduction to Modern Statistical Mechanics. New York: Oxford University Press, 1987.
- [28] Aruksakunwong, O., and others. On the lower susceptibility of oseltamivir to influenza neuraminidase subtype N1 than those in N2 and N9. Biophys. J. 92 (2007): 798–807.
- [29] Malaisree, M., Rungrotmongkol, T., Decha, P., Intharathep, P., Aruksakunwong, O., and Hannongbua, S. Understanding of known drug-target interactions in the catalytic pocket of neuraminidase subtype N1. Proteins. 71 (2008): 1908–1918.
- [30] Case, D.A., and others. Amber 10 Sanfrancisco: University of California, 2008.
- [31] Duan, Y., and others. A point-charge force field for molecular mechanics simulations of proteins based on condensed-phase quantum mechanical calculations. J. Comput. Chem. 24 (2003): 1999–2012.
- [32] Jorgensen, W.L., Chandrasekhar, J., Madura, J.D., Impey, R.W., and Klein, M.L. Comparison of simple potential functions for simulating liquid water. J. Chem. Phys. 79 (1983): 926–935.
- [33] Udommaneethanakit, T., Rungrotmongkol, T., Bren, U., Freceer, V., and Stanislav, M. Dynamic behavior of avian influenza A virus neuraminidase subtype H5N1 in complex with Oseltamivir, Zanamivir, Peramivir, and their phosphonate Analogues, J. Chem. Inf. Model. 49 (2009): 2323–2332.
- [34] Arsawang, U., and others. How do carbon nanotubes serve as carriers for gemcitabine transport in a drug delivery system?. J. Mol. Graph. Model. 29 (2011): 591–596.
- [35] Frisch, M.J., and others. Gaussian 03 Revision C. 02. Wallingford CT: Gaussian Inc., 2004.

- [36] Wang, J., Wolf, R.M., Caldwell, J.W., Kollman, P.A., and Case, D.A. Development and testing of a general amber force field. J. Comput. Chem. 25 (2004): 1157–1174.
- [37] Ryckaert, J.P., Ciccotti, G., and Berendsen, H.J.C. Numerical integration of the Cartesian equations of motion of a system with constraints: molecular dynamics of n-alkanes. J. Comput. Phys. 23 (1997): 327–341.
- [38] York, D.M., Darden, T.A., and Pedersen, L.G. The effect of long-range electrostatic interactions in simulations of macromolecular crystals: a comparison of the Ewald and truncated list methods. J. Chem. Phys. 99 (1993): 8345–8348.
- [39] Malaisree, M., and others. Source of oseltamivir resistance in avian influenza H5N1 virus with the H274Y mutation. Amino. Acids. 37 (2009): 725-32.
- [40] Rungrotmongkol, T., and others. Molecular insight into the specific binding of ADP-ribose to the nsP3 macro domains of chikungunya and Venezuelan equine encephalitis viruses: molecular dynamics simulations and free energy calculations. J. Mol. Graph. Model. 29 (2010): 347-53.

VITAE

Name; Wasinee Khuntawee

Date of birth; February 15th, 1987

Place of birth; Nakorn Sawan, Thailand

Nationality; Thai

E-mail address; waryvanilla@hotmail.com, wasinee.k@student.chula.ac.th

EDUCATION;

2009-2010; Master degree (M.Sc.) in chemistry;

Faculty of science, Chulalongkorn University, Bangkok, Thailand

2005-2009; Bachelor degree (B.Sc.) in chemistry;

Faculty of science, Silpakorn University, Nakhon Pathom, Thailand